ADVANCED HEALTHCARE MATERIALS
www.advhealthmat.de

Water-Mediated On-Demand Detachable Solid-State Adhesive of Porous Hydroxyapatite for Internal Organ Retractions

Masahiro Okada, Shi Chao Xie, Yusuke Kobayashi, Hiroaki Yanagimoto, Daisuke Tsugawa, Masaru Tanaka, Takayoshi Nakano, Takumi Fukumoto, and Takuya Matsumoto**

Novel adhesives for biological tissues offer an advanced surgical approach. Here, the authors report the development and application of solid-state adhesives consisting of porous hydroxyapatite (HAp) biocompatible ceramics as novel internal organ retractors. The operational principles of the porous solid-state adhesives are experimentally established in terms of water migration from biological soft tissues into the pores of the adhesives, and their performance is evaluated on several soft tissues with different hydration states. As an example of practical medical utility, HAp adhesive devices demonstrate the holding ability of porcine livers and on-demand detachability in vivo, showing great potential as internal organ retractors in laparoscopic surgery.

1. Introduction

Laparoscopic surgery has become the gold standard for surgical management of diseases in the reproductive (particularly gynecological) and digestive system (as for cholecystectomy) owing to multiple benefits compared with open surgery, such as less blood loss, shorter hospital stay, faster recovery of bowel movement with a shorter f to first flatus, and less serious perioperative complications including surgical site infections.[1] However, it is still challenging to expose the operative field during laparoscopic surgery.[2] For example, in upper-gastrointestinal (GI) surgery, a retraction of the liver is crucial because the lesser curvature of the stomach is covered by the left lobe of the liver. The current retraction techniques involving mechanical gripping, hanging, or suturing with notched forceps, thin slings/tubes, or sutures/stitches,[3] have a potential risk of damaging the liver, causing lacerations and crush injury.[4] In addition, these physical retraction techniques are time-consuming, and the average time required for liver retraction is 2.8–8.6 min.[3] Therefore, a safe and convenient internal organ retraction method/device is urgently needed for the next generation of laparoscopic surgery.

An appealing alternative to mechanical retractors might be the use of soft tissue adhesives such as cyanoacrylate,[5] gelatin-resorcinol-formaldehyde/glutaraldehyde (GRFG),[6] and fibrin[7] glues. These commercially-available glue-type adhesives are convenient for applying the entire target area, eliminating stress localization that would reduce tissue damages during the retraction.[8] However, these adhesives have not been used for internal organ retraction in clinical practices because cyanoacrylate and GRFG show specific toxicity, and fibrin lacks adhesion strength.[9] Researchers have developed unique adhesives with high adhesion strength using biocompatible polymers such as hydrophobically-modified gelatin,[10] dissipative hydrogels coupled with bridging polymers,[11,12] and mussel-inspired adhesives containing dihydroxyphenyl groups.[8] Solid-state adhesives such as gecko-inspired tapes,[13] octopus-inspired nanosucker arrays,[14] and silica nanoparticle dispersions[15] have also been developed. However, the above adhesives have another potential risk of damaging when the adhesive is detached forcibly (due to

M. Okada, S. C. Xie, Y. Kobayashi, T. Matsumoto
Department of Biomaterials, Faculty of Medicine, Dentistry and Pharmaceutical Sciences
Okayama University
2-5-1 Shikata-cho, Kita-ku, Okayama City, Okayama 700-8558, Japan
E-mail: m_okada@cc.okayama-u.ac.jp; tmatsu@md.okayama-u.ac.jp
H. Yanagimoto, D. Tsugawa, T. Fukumoto
Division of Hepato-Biliary-Pancreatic Surgery, Department of Surgery
Kobe University Graduate School of Medicine
7-5-2 Kusunoki-Cho, Chuou-Ku, Kobe City, Hyogo 650-0017, Japan
M. Tanaka
Soft Materials Chemistry, Institute of Material Chemistry and Engineering, Department of Applied Chemistry, Graduate School of Engineering
Kyushu University
744 Motooka, Nishi-ku, Fukuoka City, Fukuoka 819-0395, Japan
T. Nakano
Division of Materials and Manufacturing Science, Graduate School of Engineering
Osaka University
2-1 Yamadaoka, Suita City, Osaka 565-0871, Japan

The ORCID identification number(s) for the author(s) of this article can be found under https://doi.org/10.1002/adhm.202304616

DOI: 10.1002/adhm.202304616

high adhesive strength) after the surgery. Therefore, a novel technology to control adhesive strength (i.e., on-demand detachability) is desired.

Calcium phosphates such as hydroxyapatite (HAp) and octacalcium phosphate (OCP) are biocompatible and they have long been used as implants or substitute materials for hard tissues in orthopedics and dentistry. Recently, we showed that porous HAp[16] and OCP[17] plates could be used as solid-state adhesives for wet soft tissues.[18] Although these porous solid-state adhesives have potential use as adhesive liver retractors, there are no data on the adhesiveness of these solid-state adhesives on the liver. Furthermore, our previous report[16] revealed that water in the adherend was migrated (i.e., absorbed) into the HAp plate, and a condensed layer of organics was formed on the tissue surface contacting the HAp plate. We hypothesized that the migration of water from the adherend into porous solid-state adhesives would be related to their adhesiveness. In general, the absorption rate of a liquid depends on the pore size,[19] and the absorption amount of a liquid depends on the open porosity of porous materials. In addition, the hydration state of adherend would also influence the water migration. Therefore, this study examined the effects of the porous structure (i.e., pore size and porosity) of HAp adhesives on the adhesion strength of soft tissues in different hydration states. We also evaluated the HAp adhesive as an internal organ retractor and demonstrated the on-demand adhesion/detachment of the HAp adhesive retractor on a porcine liver in vivo.

2. Results and Discussion

2.1. HAp Plates with Different Porous Structures

An aqueous dispersion of low-crystallized HAp nanoparticles (particle size, 43 nm; solid content, 6.0 wt%) was prepared according to the previous report.[16] The dispersion was a viscous liquid because a network structure of HAp nanoparticles formed by particle–particle interactions[20] owing to zwitterionic-charged surfaces consisting of Ca^{2+}, PO_4^{3-}, and OH^-. After the dispersion was dried to prepare the plate, nanosized pores were generated by the nanoparticle network structure in the plate. In this study, no binder molecules such as water-soluble polymers, which adsorb and cover the HAp surface, were used to prepare plates. Typically, HAp plates ($5 \times 5 \times 1$ mm^3) were prepared by drying the dispersion in a mold ($10 \times 10 \times 1$ mm^3) at 60 °C. Heat treatments were conducted to change the porous structure of the plates (**Figure 1A**).

When the treatment temperature was below 800 °C, the HAp plate did not shrink significantly (Figure 1B) and hence the porosity did not change significantly (Figure 1C). Conversely, the pore size increased significantly (Figure 1D) because of the local densification of the pore wall due to the crystallization of HAp (Figure S1A, Supporting Information).[21] The increase in the pore size was accompanied by a decrease in the specific surface area (Figure 1E). The SEM observation also revealed the increase in pore size at the surface (Figure 1F).

The heat treatment above 1000 °C induced a significant shrinkage (Figure 1B) with a reduction in porosity (Figure 1D) and pore size (Figure 1E) due to the sintering of crystals (Figure S1B, Supporting Information). The final size of each HAp plate ($5 \times 5 \times 1$ mm^3) was adjusted by changing the initial mold size calculated from the linear shrinkage by the heat treatment. The heat treatment of the HAp plate improved its flexural strength from 4 to 70 MPa (Figure S1C, Supporting Information).

2.2. Effect of Pore Structure on Immediate Adhesion

Ex vivo shear adhesion tests (Figure 1G) were conducted at 30 s after contacting the samples onto mouse dermis to quantitatively evaluate the immediate soft tissue adhesion, wherein chemical and physical interactions were involved without considering cellular functions due to the short contact time. The apparent shear adhesion strength did not change after the heat treatment at 600 °C and decreased as the heating temperature increased (Figure 1H). The histological sections of the mouse dermis contacting the HAp plates indicated the condensation of the tissue matrix near the HAp surface (Figure 1I), and the thickness of the condensed layer decreased as the heating temperature increased (Figure 1J). The dense (i.e., highly-sintered) HAp plates prepared at high temperature did not show significant tissue condensation or adhesion (Figure 1H,J). The shear adhesion strength of the mouse dermis showed the highest correlation to the porosity ($R^2 = 0.9101$) of HAp plate and the condensed layer thickness ($R^2 = 0.9196$) of the tissue (Figure S3, Supporting Information). Considering that the condensed layer on the tissue surface was formed by water capillary action from tissues into the pores of HAp plates, the water absorption would be the key factor for the immediate adhesion of porous solid-state adhesives.

The water absorption behaviors of various HAp plates were studied by placing a droplet of pure water or cell culture medium on the plate and recording the images using a high-speed camera (Figure S2A, Supporting Information). When the heat treatment temperature was below 800 °C, the water absorption rate increased with temperature (Figure S2B, Supporting Information) because of the increased pore size (Figure 1E) at the same porosity (Figure 1D), which is consistent with the Washburn capillary rise equation.[19] The water absorption rate decreased above 800 °C (Figure S2B, Supporting Information) due to the significant reduction in porosity (Figure 1D). Because HAp plates with different pore sizes at the same porosities (prepared below 800 °C) did not cause a significant difference in the immediate shear adhesion strength for soft tissues (Figure 1E), it implied that the porosity (i.e., water absorption capacity) was more important than the pore diameter (i.e., water absorption rate). This would be because the water absorption rate was sufficiently high, even for the small pore size in this experimental condition. Of note, these results suggest that the adhesion strength of HAp plate would be enhanced by increasing its porosity, which could be achieved by using polymer bead or sponge templating methods.[22] The HAp plate could absorb not only pure water but also cell culture media containing organics and inorganics (Figure S2B, Supporting Information) and water in the tissues (Figure S2D–G, Supporting Information). The adsorption rate of these solutions decreased compared to that of pure water, which could be due to the surface-active organics in the solutions.

2.3. Immediate Adhesion for Different Soft Tissues

In the following experiments, the HAp plate heated at 600 °C was used as the HAp adhesive. To reveal the adhesion mechanism

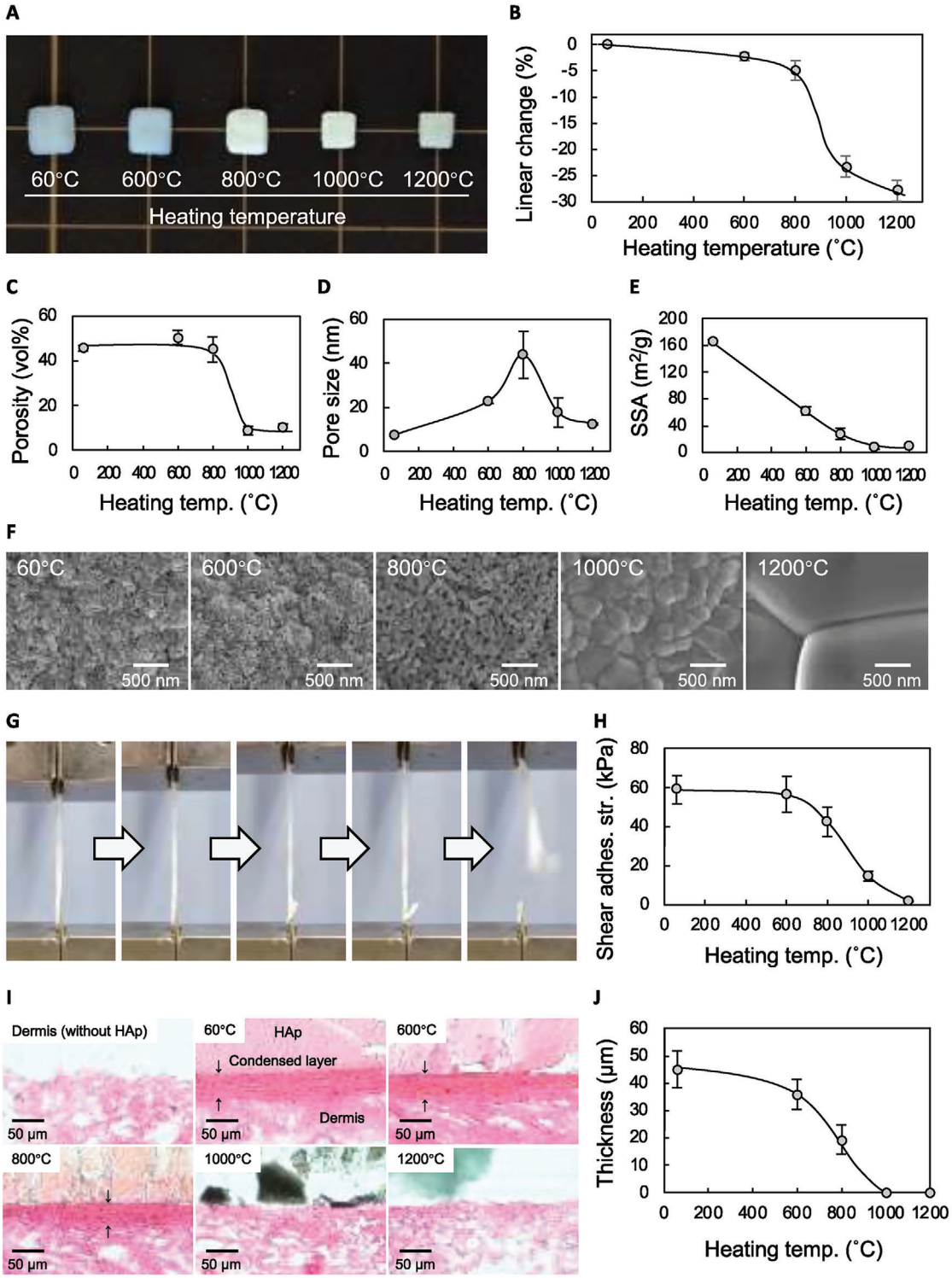

Figure 1. Preparation and characterization of HAp with different porous structures. A) Digital photographs of HAp plates after heat treatments at different temperatures. B) A linear shrinkage of HAp plates after the heat treatments ($N = 3$). C) Porosity, D) pore size, and E) specific surface area (SSA) of HAp plates after the heat treatments, determined using mercury intrusion porosimetry ($N = 3$). F) SEM images of HAp plates showing the porous structures. G) Digital photographs taken during shear adhesion test using a mouse dermis. H) Apparent shear adhesion strengths of HAp plates with different porous structures ($N = 5$). I) Histological sections of mouse dermis before and after contacting the HAp plates, showing condensed layers (indicated with arrows) at the surfaces contacted with porous HAp plates. J) Condensed layer thickness of mouse dermis after contacting HAp plates after heat treatments at different temperatures ($N = 5$). Error bars indicate standard deviations.

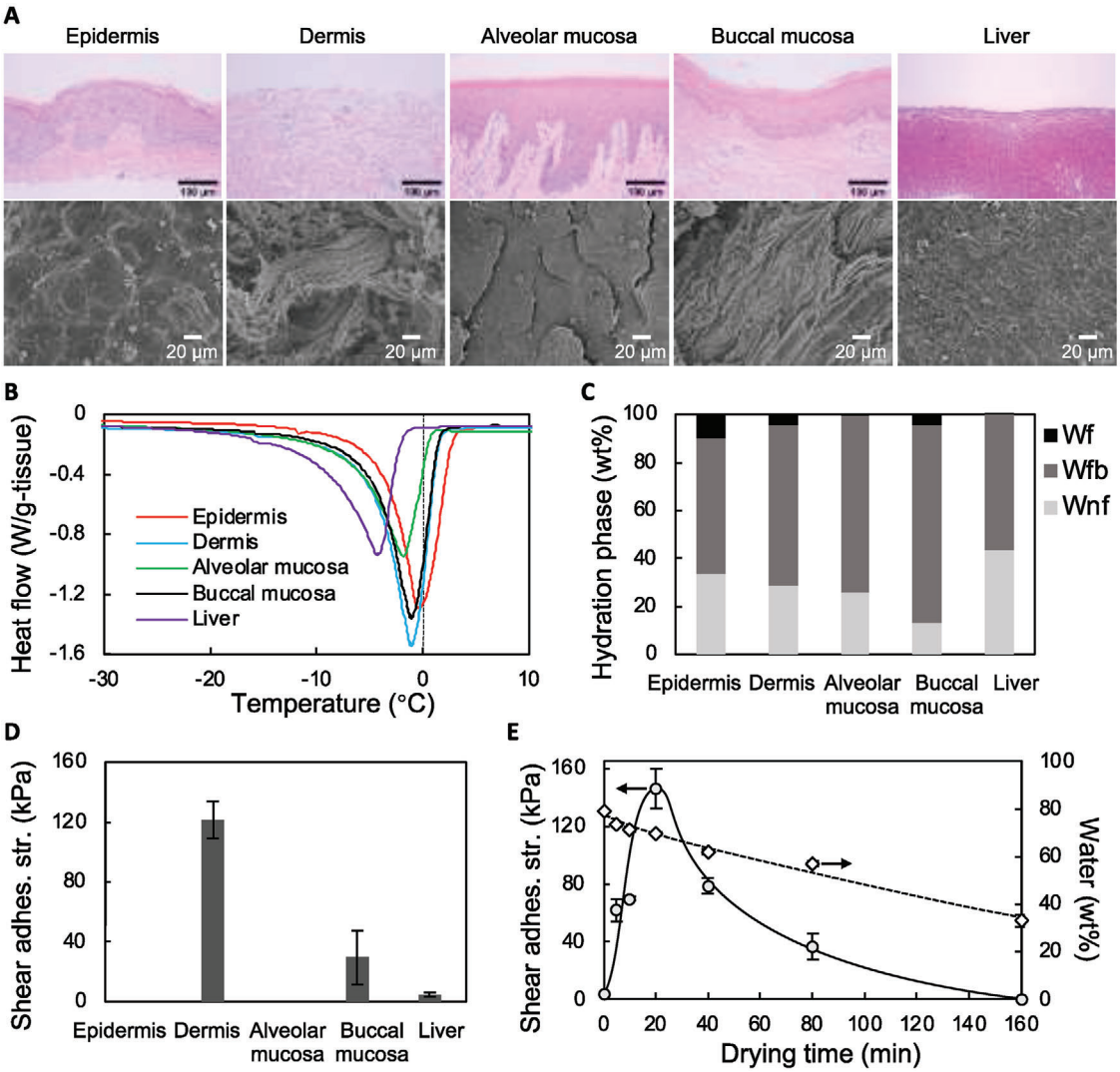

Figure 2. Adhesion properties of porous HAp plates onto various tissues. A) H&E-stained sections and SEM images of porcine tissues: epidermis, dermis, alveolar mucosa, buccal mucosa, and liver. B) Representative DSC heating curves of the porcine tissues, showing the melting of frozen water below 0 °C. C) Contents of free water (W_f), freezing bound water (W_{fb}), and non-freezing bound water (W_s) of porcine tissues. D) Apparent shear adhesion strengths of HAp plates treated at 600 °C on porcine tissues ($N = 5$). E) Variations of water content and apparent shear adhesion strength of HAp plates treated at 600 °C on wet porcine tissues during drying in the air ($N = 3$). Error bars on each graph indicate standard deviations.

in detail, different porcine tissues were used as adherends because porcine tissues have a larger size than mouse tissues used in the preliminary tests described earlier and show more similarity with human tissues. The tissues used in this study included the epidermis, dermis, alveolar mucosa, buccal mucosa, and liver (**Figure** 2A). The epidermis (dry surface) and the alveolar mucosa (wet surface) have keratinized stratum corneum layers. The buccal mucosa (wet surface) contains a layer with a low degree of keratinization, and the dermis (wet surface) is free of keratinized layers. In addition, the retraction target, liver, was also used in this study. The liver is covered with Glisson's capsule consisting of collagen and the serous membrane that comprises a single layer of mesothelial cells.[23] The liver used in this study was the left medial lobe of drained liver.[24]

As described in the previous subsection, the water migration from the tissue to the HAp plates would be a key factor for immediate adhesion. Therefore, the water content (Figure S4A, Supporting Information) and the hydration structure (Figure 2B,C) of each tissue were evaluated. The hydration structure on polymer and ceramic biomaterials has been characterized into three distinct types (i.e., free water, intermediate water, and bound water) depending on the interaction between them.[25,26] These structures can be distinguished using nuclear magnetic resonance (NMR), differential scanning calorimetry (DSC), and Fourier-transform infrared spectroscopy (FT-IR). Free water has no interaction with polymer chains. It shows a short NMR correlation time (t_c) value of 10^{-12}–10^{-11} s similar to bulk water, an O–H stretching vibration at around 3200 cm^{-1} in FT-IR, and a crystallization/melting at 0 °C in DSC. Freezing-bound water (i.e., intermediate water) interacts weakly with polymer chains. It exhibits lower mobility with a t_c value of 10^{-10}–10^{-9} s, a stretching vibration around 3400 cm^{-1}, and a crystallization/melting below

0 °C. Non-freezing water (i.e., bound water) interacts strongly with polymer chains. It shows much lower mobility with a t_c value of 10^{-8}–10^{-6} s, a stretching vibration around 3600 cm^{-1}, and no crystallization is detected in DSC even at −100 °C. Of note, intermediate water has fundamental importance in the protein adsorption capacity of polymer surface.[27] Although intermediate water is also presented in biopolymers such as cross-linked gelatin gels,[28] there is no report on the hydration structure of biological tissues. To estimate the hydration structures in porcine tissues, DSC measurements were conducted for porcine tissues frozen at −100 °C (Figure 2B and Figure S4B, Supporting Information). In each DSC heating curve, an endothermic peak was observed below 0 °C, indicating the presence of intermediate water in biological tissues. The endothermic peak above 0 °C was counted as free water. The three hydration structures were detected, and free water content was the least in all the tissues (Figure 2C). The intermediate water was the largest in content, and its content and melting point were different among the tissues (Figure 2B,C). These results indicate that the hydration structure depends on the composition of the tissue (Figure S4A, Supporting Information). For example, by comparing the dermis and the buccal mucosa with the same lipid contents, the buccal mucosa with less protein (i.e., more polysaccharides) had more intermediate water. In addition, by comparing the buccal mucosa and the liver with the same protein contents, the liver with more lipids had more non-freezing bound water. It would be because ice structure tended to form around the hydrophobic component of the lipid and/or strong interactions were involved between water and the ionic head groups in the lipid bilayers.[29]

The shear adhesion tests on different tissues (Figure 2D) show that the HAp plates did not adhere to the epidermis and alveolar mucosa with keratinized stratum corneum layers. Additionally, the shear adhesion strength on the buccal mucosa with a low degree of keratinization was significantly smaller than that on the dermis without keratinized layers. These results confirm the importance of water migration from tissues into HAp plates for immediate adhesion. When comparing the tissues without keratinized layers, the shear adhesion strength on the dermis with more intermediate water was higher than that on the liver with more non-freezing bound water. Attenuated total reflection (ATR) FT-IR measurements of tissue surfaces revealed the decrease in intermediate water content after the attachment of HAp, which was accompanied by the condensation of organics on the tissue surface (Figure S5, Supporting Information). This result indicates that the mobility water interacting with biomolecules would influence the water migration from tissues into HAp plates. Of note, the low shear adhesion strength onto the liver should also be related to the strength of the liver itself (i.e., the tensile strength of the human liver capsule is reported to be 10 kPa,[30] which was almost the same value as the tensile adhesion strength of porcine liver onto HAp plates shown in Section 2.4). Therefore, to separate the effect of the water from the other factors, the same dermis with different water contents was used as adherends. First, an intact porcine dermis was immersed in a saline to create an initial state containing more water (80 wt%; Figure 2E) than the intact state (68 wt%; Figure S4A, Supporting Information). The water content and the shear adhesion strength were measured after the dermis was dried in air (Figure 2E). At the initial state when the water content was 80 wt%, the shear adhesion strength was almost zero. The shear adhesion strength increased to 146 kPa when the water content decreased to 70 wt%, where free water was almost negligible (Figure 2C). Further drying reduced water content and led to lower shear adhesion strength.

From the aforementioned results, the mobility of water (i.e., hydration structure) in tissues should impact the adhesion of the porous solid-state adhesives (**Figure 3**A). First, the capillary action enhanced the macroscale close contact between the tissue and HAp plate. Second, the number of molecular scale interaction between the HAp and matrix organic molecules (such as collagen) increased by the increased concentration (i.e., condensation) of matrix organics. Regarding the molecular scale interaction, the collagen triple helix exposes carbonyl groups on the surface that can interact electrostatically with calcium ions on the HAp surface.[31] Besides, the dehydration of tissues can induce salting-out and collagen aggregation[32] or the disruption of the triple helix (depending on their amino acid sequence[33]). The hydrophobic moieties are exposed and contribute to the hydrophobic interaction of HAp modified by the adsorption of lipids[34] from the tissue. Therefore, the adhesion strength would be enhanced by the surface modification of HAp with amphiphilic molecules[35] or low-energy electron irradiation.[36] Rose and coworkers showed that a strong and rapid adhesion between two hydrogels can be achieved using nanoparticulate adhesives, and they claimed that the adhesiveness depends not only on the ability of nanoparticles to adsorb onto polymer gels but also the ability of polymer chains to reorganize dissipate energy under stress when adsorbed onto nanoparticles.[15] Third, the dehydration after contacting with the HAp plate would increase the stiffness of the tissue surfaces because the water provides a lubricating effect in collagen fibrils,[37] and the increased stiffness would increase the adhesion strength. An additional effect of the water migration would be the viscosity change of the water layer at the interface of HAp and tissues. For example, Kurihara et al. showed that the presence of water at the single molecule level made the mica adhere 12 500 times stronger than in the presence of thicker water layer.[38]

Based on the above adhesion mechanism, the adhesion strength can be controlled by changing the water hydration structure of tissues, and the shear adhesion strength decreased to approximately one-fifth by adding 10 µL of water to one HA plate adhering on the tissues (Figure 3B). The decreased adhesion strength would be caused by re-hydration of tissues. After water addition, the residual adhesion forces could be detected, which would be due to the molecular scale interaction between the HAp and matrix organic molecules (such as collagen). The HAp adhesive demonstrated advantageous features as an internal organ retractor because it has sufficient adhesive strength and is detachable without damaging the tissue after surgery. Therefore, the feasibility of the HAp adhesive as a liver retractor was assessed.

2.4. HAp Adhesive for Liver Retraction

First, the feasibility of the HAp adhesive as a liver retractor was assessed qualitatively using a mouse liver (Movie S1, Supporting Information). The HAp plate adhered to the mouse liver immediately after the contact, and the liver could be retracted by moving the HAp plate. The HAp plate adhered to the mouse liver could be

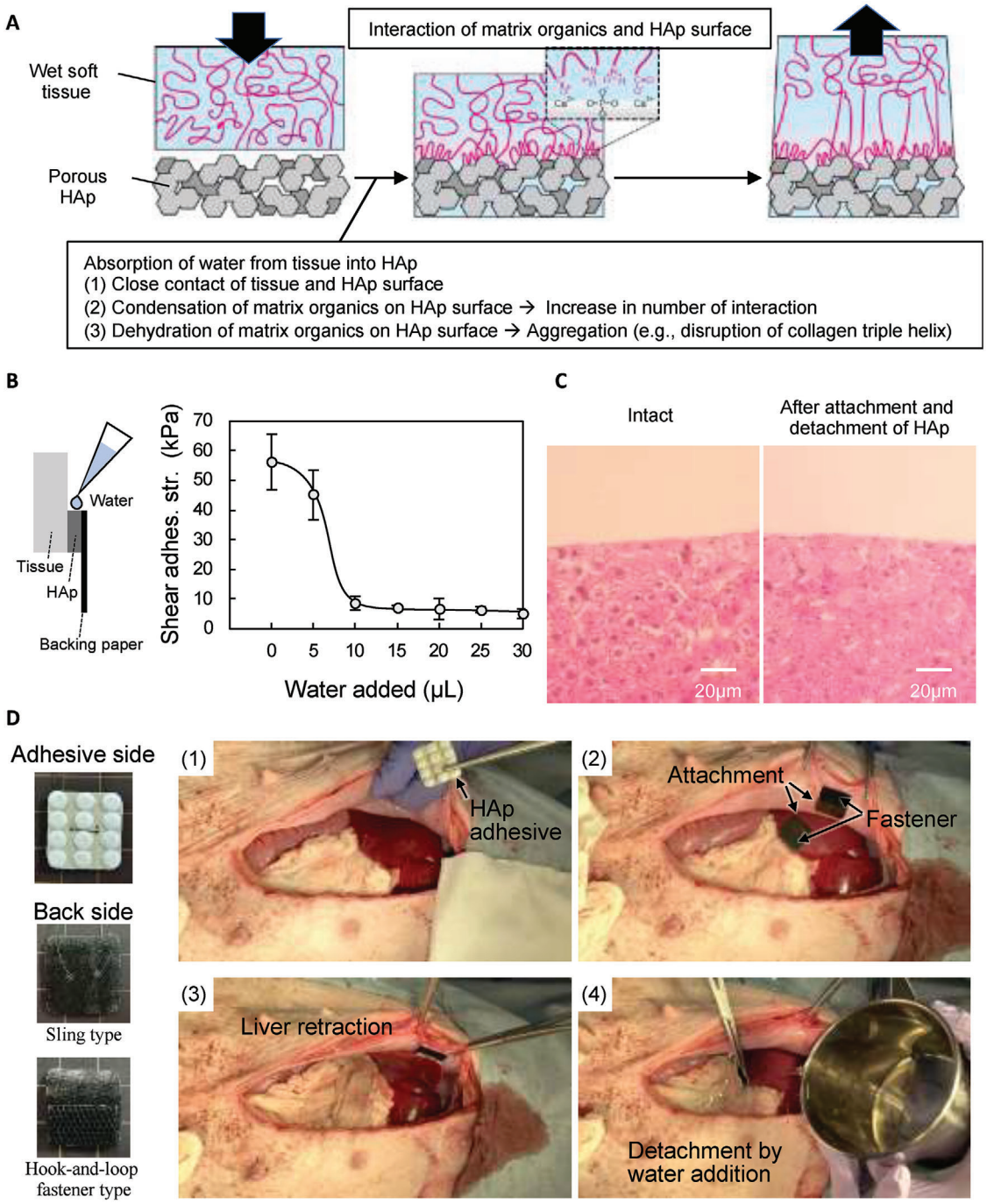

Figure 3. HAp adhesives as an internal organ retraction. A) Proposed mechanism of immediate adhesion of soft tissues on porous HAp plate. B) Detachment of HAp plates on mouse dermis by adding water. C) H&E-stained sections of mouse livers before and after the attachment of the HAp plate followed by detachment by adding water. D) A prototype retractor device made with HAp plate array and sequential photographs of porcine liver retraction and detachment of the prototype device. Two retractor devices were attached to the liver and the peritoneum, respectively and fixed by hook-and-loop fasteners. After usage, the devices were detached from the tissues by adding water.

removed by adding water. The amount of water added influenced the detachment force (Figure 3B). The histological evaluation of the liver showed no noticeable change in cell morphologies after the HAp attachment, followed by detachment with adding water (Figure 3C).

Next, the HAp adhesive was assessed using porcine liver ex vivo and in vivo. Because the immediate adhesion strength of a HAp plate was 10.8 ± 1.0 kPa on the porcine liver in the tensile mode (Figure S6, Supporting Information), an adhesive device consisting of an array of HAp plates was prepared as a liver retrac-

tor (Figure 3D). Using a total of 48 HAp plates, the 192-g porcine liver could be lifted ex vivo (Figure S7 and Movie S2, Supporting Information). The failure analysis after the tensile adhesion tests revealed that the HAp surface was covered with membranes after forced detachment from the liver without water addition (Figure S6, Supporting Information). In contrast, the area covered with the membranes decreased after detachment with water addition, reflecting the decreased adhesion strength by water addition. Of note, proteomic analysis of the membrane on HAp with and without water addition could help to understand the molecular-level interaction between HAp and the target tissues.

In the case of liver retraction, it is not necessary to lift the whole liver, and 12 plates were used in vivo to retract the porcine liver (Figure 3D; see also Movie S3, Supporting Information). After applying another adhesive device on the peritoneum and combining the device on the liver with the hook-and-loop fasteners on the back, it was possible to keep the liver retraction. By adding saline, these devices could be easily detached from the organs in vivo. No liver damages such as lacerations and crush injury were observed, and the liver capsule remained intact after the in vivo experiment on the porcine liver.

Commercially available soft tissue adhesives have not been used in clinical practice for internal organ retraction because of their toxicity or low adhesion strength.[9] Although biocompatible adhesives have been developed, these adhesives would have another risk of organ injury when the retracted organs are peeled forcibly from the adhesives after the surgery. Recently, on-demand detachable adhesives were developed by utilizing the temperature-induced sol-gel transition[39] and light-induced decomposition.[40] Compared with these adhesives, the solid-state adhesive HAp retractor developed in this study has advantages, such as no time-consuming setting reaction for the adhesion of HAp and easy detachment of HAp without decomposed products. In addition, HAp materials are biocompatible and have been used clinically for many years, and in this study, no liver damage was observed in the in vivo experiments with porcine livers. Further evaluation of the mechanical and biological safety of the porous HAp retractor, including the effect on liver function, is required for clinical applications because immediate adhesion involves dehydration of tissue surfaces. To use the porous HAp retractor in laparoscopic surgery, it is also necessary to optimize the device shape design to reduce the operation time for liver retraction.

3. Conclusions

This study examined the effects of the porous structure (i.e., pore size and porosity) of HAp adhesives on the adhesion strength of soft tissues with different hydration states. For the mouse dermis, the porosity of the HAp adhesive showed a higher correlation with the shear adhesion strength than that with the pore size. When comparing the tissues without keratinized layers, the shear adhesion strength on the tissue with more intermediate water was higher than that on the tissue with more non-freezing bound water. The water content of dermis also changed the shear adhesion strength of HAp adhesives. We also evaluated the HAp adhesive as an internal organ retractor, and demonstrated the on-demand adhesion/detachment of the HAp adhesive retractor on a porcine liver in vivo.

4. Experimental Section

Materials: Unless otherwise mentioned, all materials were of reagent-grade and used as received from FUJIFILM Wako Pure Chemical Corporation (Osaka, Japan). Milli-Q water (Millipore Corp., Bedford, MA, USA) with a specific resistance of 18.2×10^6 Ω·cm was used.

HAp-Nanoparticle Dispersions and Plates: An aqueous dispersion of HAp nanoparticles was prepared according to the method described in a previous study.[41] Briefly, an aqueous solution of calcium nitrate (42 mM, 800 mL) was poured into a 1 L reactor and its initial pH was adjusted to 10 by adding a 28% ammonia solution under stirring. An aqueous solution of diammonium phosphate (100 mM, 200 mL) was added to the reactor at room temperature (≈20 °C). The resulting mixture was stirred for another 24 h, then centrifuged and washed until the pH of the solution became neutral.

The aqueous dispersion of HAp (6 wt%) was degassed, and 400 µL of the dispersion was transferred to a polypropylene (PP) mold (10 mm × 10 mm × 0.3 mm). Once the dispersion was dried in the mold at 60 °C for 24 h, a HAp plate was obtained. The dried HAp plate was then heated from room temperature to a predetermined temperature (600, 800, 1000, or 1200 °C) at a heating rate of 10 °C min^{-1} and maintained at the temperature for 1 h. The heater of the furnace was automatically turned off after 1 h, and the sample was naturally cooled in the furnace to room temperature. The resulting heat-treated samples were used without further purification.

Basic Characterizations of HAp Plates: The linear shrinkage after the heat treatment was determined from digital photographs before and after the treatment using an image analysis software (Image J; NIH, MD, USA). Five measurements were conducted for each sample, and the average value was calculated.

Three-point flexural strengths of the samples were measured on a universal testing machine (Ez-test; Shimadzu Corp., Kyoto, Japan) equipped with a load cell of 500 N at a span of 3.0 mm at a loading rate of 0.5 mm min^{-1}. The thickness of each sample was measured with a micrometer (MDC-25 MJ; Mitutoyo Corp., Kanagawa, Japan). Five measurements were conducted for each sample, and the average value was calculated.

The surface morphology of the film was observed with a scanning electron microscope (SEM, JSM-6701F; JEOL Ltd., Tokyo, Japan) at the Central Research Laboratory in Okayama University Medical School. The dried sample was loaded onto an aluminum stub and coated with osmium (Neoc-Pro, Meiwafosis Co. Ltd., Tokyo, Japan).

The porosities, pore-size distributions, and specific surface areas were determined using mercury intrusion porosimetry (AutoPore IV 9520; Micromeritics Instrument Corp., Norcross, GA) after the samples were dried under vacuum at 60 °C for 24 h. Three measurements were conducted for each sample, and the average value was calculated.

Crystallographic analysis was conducted by X-ray diffraction (XRD, RINT2500HF; Rigaku Corp., Tokyo, Japan) using Cu-Ka (1.54 Å) irradiation at 40 kV and 200 mA. The samples were scanned from 20° to 45° at a scan speed of 2° min^{-1}.

In Vitro Mouse Dermis Attachment (Adhesion) and Detachment: All the animal procedures using mice were strictly in accordance with the Guidelines for Animal Experiments at Okayama University after the approval of the experimental protocol by Okayama University (OKU-2020530).

The shaved skin tissues were excised from the back of 6-week-old male BALB/c mice (Japan SLC, Inc., Shizuoka, Japan) after being euthanized with CO_2 gas or an overdose of isoflurane. The reticular dermal layer was exposed by removing the superficial fascia, trimmed into 5 mm × 40 mm strips, immersed in a saline solution (0.9 w/v% NaCl solution), and used within 1 day after isolation. After the saline solution on the trimmed tissues was removed with filter papers, the HAp plate fixed on a piece of thick paper with double-side tape was attached to the tissue with an overlapping area of 5 mm × 5 mm, as reported previously.[42] Shear adhesion tests were performed with a mechanical tester (Ez-test; Shimadzu Corp.) at a speed of 150 mm min^{-1} after contacting HAp plates for 30 s. The apparent shear adhesion strength was calculated from the maximum load (fracture force) divided by the overlapping area ($N = 5$). The detachment was evaluated by measuring the shear adhesion strengths

after adding water (5–30 µL) at the interfaces of HAp plates and tissues ($N = 5$).

For the measurement of condensed layer on mouse dermis, the tissues before and after contacting HAp plates for 30 s were embedded in a cryosection medium, and immediately frozen thereafter. The cryosections used in this study were obtained according to a previously reported method using adhesive films.[43] with a cryomicrotome (CM-3050S, LEICA). These sections were then fixed with paraformaldehyde and stained with eosin before being observed under a microscope.

Evaluation with Porcine Soft Tissues: The relationship between the tissue characteristics and the shear adhesion strength of HAp plates (after heating at 600 °C) was evaluated by using epidermis and dermis (excised from frontal skins), alveolar mucosa, buccal mucosae, and liver of slaughtered barrow hogs (≈6-month-old; weight, 100–120 kg; Tokyo-Shibaura Zoki KK., Tokyo, Japan).

For histological and SEM observation, each tissue was fixed with a solution of 2% paraformaldehyde and 2% glutaraldehyde followed by 2% osmium tetroxide solution, dehydrated with ethanol, and then immersed in *tert*-butanol. For histological observation, the dehydrated sample was embedded in paraffin and a section was made with a microtome. The section was stained with hematoxylin and eosin (H&E) before observation under a microscope. For SEM observation, the sample was freeze-dried and then coated with osmium (Neoc-Pro).

For the composition of each tissue, weight percentages of crude proteins, total lipids, and water were measured by the Kjeldahl method,[44] Soxhlet extraction with diethyl ether[44] and gravimetric method, respectively. In the Kjeldahl procedure, after digestion in concentrated sulfuric acid, the total organic nitrogen was converted to ammonium sulfate. Ammonia was formed and distilled into a boric acid solution under alkaline conditions. The borate anions were titrated with a standard hydrochloric acid solution to calculate the content of nitrogen representing the amount of crude protein in the sample. Most proteins contained 16% nitrogen; thus, the conversion factor was 6.25.[44] The water content was calculated after the DSC measurements described below.

The phase transition of water in the intact tissue was measured under a nitrogen atmosphere using a DSC instrument (DSC-60 Plus, Shimadzu Corp.). The wet sample (≈10 mg) was weighed in a DSC aluminum pan, and then the pan was sealed hermetically. The sealed pan was first cooled down to −100 °C at the cooling rate of 2 °C min^{-1}, held at −100 °C for 1 min, and then heated to 25 °C at a heating rate of 2 °C min^{-1}. The dry sample weight was determined after the DSC measurement, after drying at 100 °C in a vacuum until the weight did not change. The amounts of different types of water in the samples were calculated by the following equations:[27]

$$W_C = (W_1 - W_0)/W_1 \quad (1)$$

$$W_C = W_{nf} + W_{fb} + W_f \quad (2)$$

$$W_{fb} = DH_{m,subzero}/334\ (J\ g^{-1}) \quad (3)$$

$$W_f = DH_{m,total}/334\ (J\ g^{-1}) - W_{fb} \quad (4)$$

where W_C is the water content; W_0 is the weight of the sample after drying at 100 °C in vacuum; W_1 is the weight of the wet sample before drying; W_{nf}, W_{fb}, and W_f are the amounts of non-freezing bound water, freezing-bound (intermediate) water, and free water, respectively; $DH_{m,\,subzero}$ and $DH_{m,\,total}$ are enthalpy changes below 0 °C and total enthalpy changes during heating, respectively.

The shear adhesion strength of the HAp plate on each porcine tissue was evaluated under the same conditions described above. The water contents of dermis under evaporating water at room temperature for different periods (0–160 min) were determined using Equation (1).

Mouse Liver Retraction: An incision was made in the middle of the abdomen of a 6-week-old male BALB/c mouse (Japan SLC, Inc.) after being euthanized with an overdose of isoflurane. An HAp plate was attached to the liver. To remove the HAp plate, 50 µL of saline was dropped onto the surface.

Ex Vivo Porcine Liver Retraction: The retractor device was fabricated by arraying the twelve HAp disks (5 mm in diameter; after thermal treatment at 600 °C) on a tape (20 × 20 mm^2 in size; Scotch DUCT-EX183M; 3M Company, Saint Paul, MN, USA). Two holes were made in the tape and a thread was threaded through the hole (Figure S7B, Supporting Information). Part of the liver (192 g) of slaughtered barrow hogs (≈6-month-old; weight, 100–120 kg; Tokyo-Shibaura Zoki KK.) was used for ex vivo retraction.

To measure the tensile adhesion strength, an HAp disk (5 mm in diameter; after thermal treatment at 600 °C) on a tape (6 × 6 mm^2 in size; Scotch DUCT-EX183M) was attached to the liver surface. As a control, a tape without HAp was also attached to the liver surface. The tensile adhesion tests were performed with a mechanical tester (Ez-test; Shimadzu Corp.) at a speed of 150 mm min^{-1}. The apparent shear adhesion strength was calculated from the maximum load divided by the attached area ($N = 5$).

In Vivo Porcine Liver Retraction: The animal procedures using swine were strictly in accordance with the Guidelines for Animal Experiments at Kobe University after the approval of the experimental protocol by Kobe University (P210606-R1).

After a pig (female; 13 weeks old; 35.3 kg) was anesthetized, an incision was made in the middle of the abdomen of the pig. A hook-and-loop fastener (pressure-sensitive AK tape; ARACOH Co. Ltd., Shizuoka, Japan) was attached to the back of retractor devices consisting of the twelve HAp disks (5 mm in diameter; after thermal treatment at 600 °C) on a tape (20 × 20 mm^2 in size; 3M Extreme Hold Duct Tape). Two devices were attached to the liver and peritoneum, respectively, and connected by the hook-and-loop fastener, so that the liver was retracted by moving the peritoneum. To remove the retractor devices, a saline (50 mL) was poured on the surfaces. After the removal, the liver damage was evaluated by gross observation.

Statistical Analysis: After the normality and homogeneity of variance were calculated using the Shapiro-Wilk and Bartlett tests, respectively, the Tukey-Kramer test was used for intergroup comparative analysis. All statistical tests were performed using R (version 3.3.2)[45] at preset alpha levels of 0.05.

Supporting Information

Supporting Information is available from the Wiley Online Library or from the author.

Acknowledgements

This work was supported by KAKENHI (grant numbers: JP20H05225, JP21K12683, JP21K18828, and JP21H03123) from Japan Society for the Promotion of Science and by CREST (grant number: JPMJCR22L5) from Japan Science and Technology Agency.

Conflict of Interest

The authors declare no conflict of interest.

Data Availability Statement

The data that support the findings of this study are available from the corresponding author upon reasonable request.

Keywords

hydroxyapatite, internal organ retractor, pore structure, soft-tissue adhesion, solid-state adhesive

Received: December 25, 2023
Revised: March 15, 2024
Published online:

[1] A. Buia, F. Stockhausen, E. Hanisch, *World J. Methodol.* **2015**, *5*, 238.
[2] C. Benzing, H. Weiss, F. Krenzien, M. Biebl, J. Pratschke, R. Zorron, *Surg. Innov.* **2017**, *24*, 186.
[3] P. Palanivelu, K. P. Patil, R. Parthasarathi, J. K. Viswambharan, P. Senthilnathan, C. Palanivelu, *J. Minimal Access Surg.* **2015**, *11*, 198.
[4] T. Nozaki, T. Kato, A. Komiya, H. Fuse, *Curr Urol* **2013**, *7*, 199.
[5] Y.-C. Tseng, H. Suong-Hyu, Y. Ikada, Y. Shimizu, K. Tamura, S. Hitomi, *J. Appl. Biomater.* **1990**, *1*, 111.
[6] S. Fukunaga, M. Karck, W. Harringer, J. Cremer, C. Rhein, A. Haverich, *Eur. J. Cardio-Thoracic Surg.* **1999**, *15*, 564.
[7] E. V. Dare, M. Griffith, P. Poitras, T. Wang, G. F. Dervin, A. Giulivi, M. T. Hincke, *Tissue Eng., Part A* **2009**, *15*, 2285.
[8] V. Bhagat, M. L. Becker, *Biomacromolecules* **2017**, *18*, 3009.
[9] M. Matsuda, M. Inoue, T. Taguchi, *J. Bioact. Compat. Polym.* **2012**, *27*, 481.
[10] A. Nishiguchi, Y. Kurihara, T. Taguchi, *Acta Biomater.* **2019**, *19*, 387.
[11] J. Li, A. D. Celiz, J. Yang, Q. Yang, I. Wamala, W. Whyte, B. R. Seo, N. V. Vasilyev, J. J. Vlassak, Z. Suo, D. J. Mooney, *Science* **2017**, *357*, 378.
[12] B. R. Freedman, A. Kuttler, N. Beckmann, S. Nam, D. Kent, M. Schuleit, F. Ramazani, N. Accart, A. Rock, J. Li, M. Kurz, A. Fisch, T. Ullrich, M. W. Hast, Y. Tinguely, E. Weber, D. J. Mooney, *Nat. Biomed. Eng.* **2022**, *6*, 1167.
[13] A. Mahdavi, L. Ferreira, C. Sundback, J. W. Nichol, E. P. Chan, D. J. D. Carter, C. J. Bettinger, S. Patanavanich, L. Chignozha, E. Ben-Joseph, A. Galakatos, H. Pryor, I. Pomerantseva, P. T. Masiakos, W. Faquin, A. Zumbuehl, S. Hong, J. Borenstein, J. Vacanti, R. Langer, J. M. Karp, *Proc. Natl. Acad. Sci. USA* **2008**, *105*, 2307.
[14] Y. C. Chen, H. Yang, *ACS Nano* **2017**, *11*, 5332.
[15] S. Rose, A. Prevoteau, P. Elzière, D. Hourdet, A. Marcellan, L. Leibler, *Nature* **2014**, *505*, 382.
[16] M. Okada, A. Nakai, E. S. Hara, T. Taguchi, T. Nakano, T. Matsumoto, *Acta Biomater.* **2017**, *57*, 404.
[17] Y. Sugiura, M. Okada, K. Hirano, T. Matsumoto, *Adv. Mater. Interfaces* **2021**, *8*, 2002032.
[18] M. Okada, T. Matsumoto, *Jpn. Dental Sci. Rev.* **2023**, *59*, 439.
[19] E. W. Washburn, *Phys. Rev.* **1921**, *17*, 273.
[20] I. R. Rutgers, *Rheol. Acta* **1962**, *2*, 305.
[21] M. Okada, K. Fujiwara, M. Uehira, N. Matsumoto, S. Takeda, *J. Colloid. Interface. Sci.* **2013**, *405*, 58.
[22] H. Yoshikawa, N. Tamai, T. Murase, A. Myoui, *J. R. Soc., Interface* **2008**, *6*, S341.
[23] I. Lua, K. Asahina, *Gut Liver* **2016**, *10*, 166.
[24] R. Michel, L. Poirier, Q. Van Poelvoorde, J. Legagneux, M. Manassero, L. Corté, *Proc. Natl. Acad. Sci. USA* **2019**, *116*, 738.
[25] M. Tanaka, T. Hayashi, S. Morita, *Polym. J.* **2013**, *45*, 701.
[26] M. Okada, E. S. Hara, D. Kobayashi, S. Kai, K. Ogura, M. Tanaka, T. Matsumoto, *ACS Appl Bio Mater* **2019**, *2*, 981.
[27] K. Sato, S. Kobayashi, M. Kusakari, S. Watahiki, M. Oikawa, T. Hoshiba, M. Tanaka, *Macromol. Biosci.* **2015**, *15*, 1296.
[28] H. Yuuki, O. Keiko, F. Kenji, T. Emiko, T. Yasuhiko, T. Masaru, *Polym. Prepr.* **2011**, *60*, 1886.
[29] M. Pasenkiewicz-Gierula, K. Baczynski, M. Markiewicz, K. Murzyn, *Biochim. Biophys. Acta, Biomembr.* **2016**, *1858*, 2305.
[30] A. Karimi, A. Shojaei, *Dig. Dis.* **2018**, *36*, 150.
[31] M. Cutini, M. Corno, D. Costa, P. Ugliengo, *J. Phys. Chem. C* **2019**, *123*, 7540.
[32] R. Komsa-Penkova, R. Koynova, G. Kostov, B. G. Tenchov, *Biochim. Biophys. Acta* **1996**, *1297*, 171.
[33] A. Naito, S. Tuzi, H. Saitô, *Eur. J. Biochem.* **1994**, *224*, 729.
[34] K. Warabino, S. Ueno, T. Hino, S. Shimabayashi, *Phosphorus Res. Bull.* **2006**, *20*, 129.
[35] Y. Li, W. Weng, *J. Mater. Sci.: Mater. Med.* **2007**, *19*, 19.
[36] D. Aronov, R. Rosen, E. Z. Ron, G. Rosenman, *Process Biochem.* **2006**, *41*, 2367.
[37] S. J. R. Kelly, R. Weinkamer, L. Bertinetti, R. L. Edmonds, K. H. Sizeland, H. C. Wells, P. Fratzl, R. G. Haverkamp, *J. Mech. Behav. Biomed. Mater.* **2019**, *90*, 1.
[38] H. Sakuma, K. Otsuki, K. Kurihara, *Phys. Rev. Lett.* **2006**, *96*, 046104.
[39] X. Shi, P. Wu, *Small* **2021**, *17*, 21012201.
[40] H. Wu, Z. Qin, X. Yu, J. Li, H. Lv, X. Yang, *J. Mater. Chem. B* **2019**, *7*, 5669.
[41] M. Okada, D. Hiramatsu, T. Okihara, T. Matsumoto, *Dent. Mater. J.* **2016**, *35*, 651.
[42] M. Okada, E. S. Hara, A. Yabe, K. Okada, Y. Shibata, Y. Torii, T. Nakano, T. Matsumoto, *Adv. Mater. Interfaces* **2020**, *7*, 1902089.
[43] T. Kawamoto, M. Shimizu, *Histochem. Cell Biol.* **2000**, *113*, 331.
[44] R. L. Bradley, *Moisture and Total Solids Analysis*, Springer, New York **2010**.
[45] R Core Team, A Language and Environment for Statistical Computing, R Foundation for Statistical Computing, Vienna, Austria, **2016**.